Nanoscale Research Letters
a SpringerOpen Journal

NANO IDEA

Ultrasound exfoliation of inorganic analogues of graphene

Václav Štengl[1*], Jiří Henych[1,2], Michaela Slušná[1,2] and Petra Ecorchard[1]

Abstract

High-intensity ultrasound exfoliation of a bulk-layered material is an attractive route for large-scale preparation of monolayers. The monolayer slices could potentially be prepared with a high yield (up to 100%) in a few minutes. Exfoliation of natural minerals (such as tungstenite and molybdenite) or bulk synthetic materials (including hexagonal boron nitride (h-BN), hexagonal boron carbon nitride (h-BCN), and graphitic carbon nitride (g-C_3N_4)) in liquids leads to the breakdown of the 3D graphitic structure into a 2D structure; the efficiency of this process is highly dependent upon the physical effects of the ultrasound. Atomic force microscopy (AFM), transmission electron microscopy (TEM), and selected area electron diffraction (SAED) were employed to verify the quality of the exfoliation. Herein, this new method of exfoliation with ultrasound assistance for application to mono- and bilayered materials in hydrophobic and hydrophilic environments is presented.

Keywords: Ultrasound; Exfoliation; Graphene inorganic analogues

Background

Mechanical exfoliation, called the 'scotch tape method' [1], was the first method used for the preparation of single-layer graphene from natural graphite. Subsequently, through the utilization of this principle, other layered materials that are so-called inorganic analogues of graphene (IAG), such as MoS_2 [2,3] and WS_2 [4], hexagonal boron nitride (h-BN) [5], hexagonal boron carbon nitride (h-BCN), and graphitic carbon nitride (g-C_3N_4) (see Figure 1), were exfoliated. The current state of knowledge about the synthesis of IAGs is gathered below.

Some recent attempts to obtain ultrathin MoS_2 include the preparation of monolayered MoS_2 flakes that were mechanically exfoliated from a piece of commercially available crystalline MoS_2 sample by the scotch tape method [6]. Joensen et al. [7] exfoliated MoS_2 into monolayers by intercalation with lithium followed by a reaction with water. Chemically exfoliated MoS_2 was also prepared via lithium intercalation using a solution of butyllithium in hexane. However, this method resulted in loss of semiconducting properties of the pristine MoS_2,
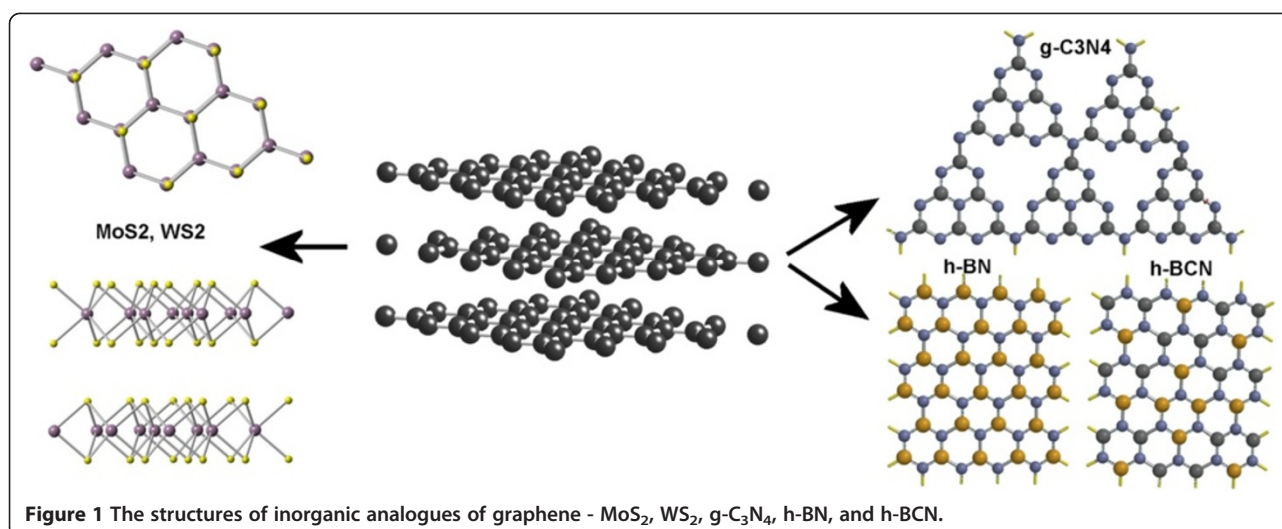
due to the structural changes that occurred during Li intercalation [8,9]. Yao et al. [10] reported on a method for the fabrication of monolayers and multilayers of BN, MoS_2, and graphene utilizing a combination of low-energy ball milling and sonication. Ball milling generates shear and compression, which can cleave the layered materials into the 2D nanosheets.

Exfoliated WS_2 was also prepared using ultrasonic treatments with *n*-butyllithium in hexane; this process was more difficult than the exfoliation of MoS_2 [8,9] due to the resistance of the WS_2 to intercalation [11,12]. Single layers of the transition metal dichalcogenides WS_2, MoS_2, and $MoSe_2$ were formed in aqueous suspensions by lithium intercalation and exfoliation of the crystalline powders [13]. Rao and Nag [14] described the preparation of WS_2 and MoS_2 sheets by lithium intercalation followed by exfoliation of the layers by ultrasonication and chemical synthesis, where molybdic acid and tungstic acid, respectively, were treated with an excess of thiourea. Another approach, a mixed-solvent strategy, exploited a low-intensity ultrasonic treatment (ultrasonic bath) for the exfoliation of MoS_2, WS_2, and BN in ethanol/water mixtures [15]. This method is suitable for the preparation of approximately 1% dispersion of exfoliated particles. Direct exfoliation of the bulk powder materials using supercritical CO_2 assisted with ultrasound also led

* Correspondence: stengl@iic.cas.cz
[1]Materials Chemistry Department, Institute of Inorganic Chemistry AS CR, v.v.i., Řež 250 68, Czech Republic
Full list of author information is available at the end of the article

Springer

Figure 1 The structures of inorganic analogues of graphene - MoS_2, WS_2, $g-C_3N_4$, h-BN, and h-BCN.

to the single and few layers of BN, MoS_2, and WS_2. The effects of supercritical CO_2 coupled with ultrasound played a key role in the exfoliation process [16]. Warner et al. [17] presented a relatively simple method to prepare thin few-layer sheets of h-BN with micrometer-sized dimensions using chemical exfoliation in the solvent 1,2-dichloroethane. Lin et al. [18] demonstrated that water is effective in the exfoliation of layered h-BN structures with the assistance of an ultrasonic bath and leads to 'clean' aqueous dispersions of h-BN nanosheets without the use of surfactants.

The h-BCN compounds were successfully synthesized by using hydrogen-free 1,3,5-trichlorotriazine and boron tribromide as reactants and metal sodium as reductant through a chemical reduction synthesis method at 450°C [19]. A facile approach has been developed to prepare B and N co-doped graphene with tunable compositions simply through the thermal annealing of graphene oxide in the presence of boric acid and ammonia [20].

Hernandez et al. [21] gathered interesting findings that included the utilization of the method of liquid-phase exfoliation, where the surface energy of the solvent was advantageously used to exfoliate graphite. The surface energy of graphene, which is approximately 70 mJ/m^2, is in the upper range of surface energies for most solvents. That would imply that this method cannot be used for the exfoliation of IAGs because the surface energies of these materials have been determined to be considerably higher than that of graphene. For example, Weiss and Phillips [22] referred that the surface energies of transition metal dichalcogenides, such as MoS_2 and WS_2, are greater than 200 mJ/m^2. Therefore, there would not be any suitable solvents, and the method of liquid-phase exfoliation could not be used for the exfoliation of IAGs.

Ultrasonic power, transferred into the liquid by means of a sonotrode (ultrasonic probe, horn), is dependent on

sonotrode shape, material, and the end load. An acoustic power of approximately 50 W/cm^2 can be transferred into water at an ambient pressure. In a well-tuned ultrasonic system, it can be assumed that the power transfer into the liquid is more than 95% of the input power, and 3% to 4% of the losses are thermal losses of the electrical components of the generator. The maximum achieved power at ambient pressure is approximately 300 W. A further increase of the ultrasonic power can be achieved by placing the ultrasonic horn in the pressurized reactor. For 1-kW power supply, the optimal pressure is approximately 4 bar; for 2 kW, a suitable pressure is approximately 6 to 7 bar. Higher pressures load the ultrasound tool too much, and the ultrasonic generator begins its inevitable falling out of resonance and its power decreases. A liquid denser than water (ethylene glycol, glycerol, etc.) also leads to a higher output power, thanks to a higher cavitation threshold.

When the liquid is exposed to intense ultrasound, the waves propagate through the liquid causing an alternating of high-pressure and low-pressure cycles that is dependent on the frequency of the electric generator. During the low-pressure cycle, high-intensity small vacuum bubbles are created, as the liquid vapor pressure is achieved. When the bubbles reach a certain size, they collapse strongly during a high-pressure cycle. During this implosion, very high pressures, high temperatures, and speed liquid jets are locally generated. This phenomenon is called cavitation [23]. The resulting hydrodynamic forces are able to disintegrate agglomerates and to mill particles in solution.

The ultrasonic vibrations are transferred into an elastic environment by spreading the longitudinal or transverse waves. Transverse waves cannot propagate in a gas or a liquid because there is no mechanism for driving the motion perpendicular to the propagation of the wave;

thus, they are transformed into standing (stationary) waves by the ultrasonic horn. Stationary waves are able to vibrate lamellar particles, using the vibration to overcome van der Waals forces. As a result, lamellar particles are gradually peeled off to reveal individual sheets. The particle milling effect is based on intense ultrasonic cavitation, while delamination is caused by stationary waves. Increasing the density of the solvent or/and increasing the pressure of the solvent will also increase the cavitation threshold [24,25]. Through the selection of suitable reaction conditions and factors (sonotrode shape, intensity of ultrasound, solvent density, pressure, etc.), it is then possible to favor the process of delamination over grinding and milling. Delamination of layered minerals [26] by ultrasound was successfully used for the preparation of exfoliated mica [27] and kaoline [28] under atmospheric pressure. Pressurized batch ultrasonic reactors were also used to exfoliate graphite to graphene [29], which then served as the precursor for the composite materials of graphene-anatase [30] and graphene oxide-anatase [31]. It can then be theorized that the exfoliation of IAGs using power ultrasound in an environment of strong polar aprotic solvents in a pressurized batch reactor could be achieved through this procedure.

In this paper, we demonstrate simple and low-cost methods for the preparation of single- and few-layered nanosheets of inorganic analogues of graphene, MoS_2, WS_2, h-BN, h-BCN, and g-C_3N_4, using stationary ultrasound waves in a pressurized ultrasonic reactor. According to the available literature, an alkaline manganate solution for the exfoliation of IAGs [32] has not been used.

Experimental

All of the chemicals used - potassium permanganate ($KMnO_4$), potassium hydroxide (KOH), hydrochloric acid (HCl), boric acid (H_3BO_3), urea ($CO(NH_2)_2$), and melamine ($C_3H_3N_6$) - were supplied by Sigma-Aldrich Company, Ltd. (St. Louis, MO, USA). The natural minerals tungstenite (WS_2) and molybdenite (MoS_2) were obtained from US Research Nanomaterials, Inc. (Houston, TX, USA) and from Rokospol Ltd. (Uherský Brod, Czech Republic), respectively.

Preparation of bulk h-BN and h-BCN

The bulk h-BN was prepared from boric acid and urea by the modified method reported by Nag et al. [33]. This chemical method allows for the control of the number of layers through the composition of the starting feedstock because the number of BN layers decreases with increasing urea content in the reaction mixture. The boric acid and urea, in a molar ratio of 1:3, were dissolved in 100 ml of water and heated at 70°C until the full evaporation of water occurred. The dried crystal powder was heated at 950°C for 5 h under a nitrogen atmosphere.

To synthesize the h-BCN bulk compound [34], boric acid was mixed with melamine in the ratio of 1:2 in an agate mortar. The mixture was then heated in a beaker at 200°C for 1 h and subsequently at 300°C for an additional 2 h. The obtained precursor was heated under a nitrogen atmosphere at 1,300°C for 5 h.

Preparation of bulk g-C_3N_4

The g-C_3N_4 was prepared by direct heating of 5 g melamine powder and was put into an alumina crucible with a cover [35]. The sample was heated at 580°C for 2 h with a heat rate of 10°C/min. After heating, a yellow powder of bulk g-C_3N_4 was obtained.

Exfoliated samples in a hydrophobic environment

Exfoliated MoS_2, WS_2, h-BN, h-BCN, and g-C_3N_4 were prepared in a large quantity from synthesized bulk samples by using a high-intensity cavitation field in a pressurized ultrasound reactor (UIP2000 hd, 20 kHz, 2,000 W, Hielscher Ultrasonics, GmbH, Teltow, Germany). A portion of 0.75 to 1 g of the bulk sample was suspended in 120 ml of appropriate aprotic solvent (N-methyl-2-pyrrolidone, N,N-dimethylformamide, or dimethyl sulfoxide) and exposed to an intense cavitation field in a pressurized batch ultrasonic reactor for 20 min. The pressure of 6 bar was set in the reactor by means of an air compressor [29]. The exfoliation led to the formation of stable suspensions in the hydrophobic (organophilic) solvents.

Exfoliated samples in a hydrophilic environment

The exfoliated IAGs stabilized in an aqueous solution were prepared through high-intensity ultrasound in a solution of $KMnO_4$ in an alkaline environment. Generally, 1 g of IAG was mixed with 120 ml of an aqueous solution of 1.5 g $KMnO_4$ and 24 g KOH in an ultrasonic reactor. The reactor was sealed and pressurized to 6 bar, and the reaction mixture was sonicated for 10 min. After irradiation, a suspension of IAG and MnO_2 in a dark green solution of K_2MnO_4 was obtained. The suspension was neutralized to a pH = 7 to 8 by adding HCl to convert all higher-valent (III, IV, VI) manganese species contents to soluble Mn^{2+}. The whole obtained reaction product was purified by dialysis using a Spectra/Por 3 dialysis membrane (Spectrum Laboratories Inc., Rancho Dominguez, CA, USA).

Chemically exfoliated bulk h-BN

The method of producing chemically exfoliated h-BN is based upon the preparation of graphene oxide [36]. In a typical experiment, 0.75 g of h-BN bulk powder was dispersed in 60 ml of 96% H_2SO_4. Subsequently, 3 g of

$KMnO_4$ was added, and the reaction mixture was stirred under heating at 40°C continuously for 6 h. The obtained pink suspension was subsequently poured onto ice and mixed with 200 ml of 30% H_2O_2. The pink squash quickly changed to a white suspension, which was washed by decantation and centrifugation until it reached a pH ~ 7.0.
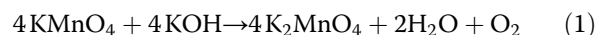
Characterization methods

Diffraction patterns were collected using a PANalytical X'Pert PRO diffractometer (Almelo, The Netherlands) equipped with a conventional X-ray tube (CuKα 40 kV, 30 mA, line focus) in the transmission mode. An elliptic focusing mirror with a divergence slit of 0.5°, an anti-scatter slit of 0.5°, and a Soller slit of 0.02 rad were used in the primary beam. A fast linear position-sensitive detector PIXcel with an anti-scatter shield and a Soller slit of 0.02 rad were used in the diffracted beam. All patterns were collected with steps of 0.013° and 500 s/step. A qualitative analysis was performed with the DiffracPlus Eva software package (Bruker AXS, Berlin, Germany) using the JCPDS PDF-2 database [37]. A water suspension of the sample material was placed onto a sample holder for transmission experiments and then covered with a Mylar foil (6 μm thick, DuPont Tejjin Films, Chester, VA, USA). Then, the second Mylar foil covers the sample to avoid losses. Finally, the sample holder was completed with a sample holder ring, making it ready for X-ray diffraction (XRD) experiments in transmission mode. The crystallite size, interlayer spacing, and number of h-BN and h-BCN layers were calculated by using the classical Debye-Scherrer equations [38,39].

Atomic force microscopy (AFM) images were obtained using a Bruker Dimension FastScan microscope. The samples for AFM measurement were prepared through the spin coating method. The samples were prepared by pipetting the exfoliated h-BN and h-BCN water suspensions onto the synthetic mica as an atomically smooth support and then were spin-coated at 6,000 rpm for 1 min. A silicon tip on a nitride lever was used with ScanAsyst (Bruker) in the air contact mode for resonance frequencies ranging from 50 to 90 kHz.

The morphology of the sample powders was inspected by transmission electron microscopy (TEM), and the crystal structure was analyzed by electron diffraction (ED) using a 300-kV JEOL 3010 (Akishima-shi, Japan). As a specimen support for the TEM investigations, a microscopic copper grid covered by a thin transparent carbon film was used. Both samples were studied in a bright field and by electron diffraction with a selecting aperture (selected area electron diffraction (SAED)) mode at an acceleration voltage of 200 kV.

Results and discussion

The method of exfoliation of IAGs in the alkaline environment is based on a process also related to the phenomena of cavitation. The reaction mixture $KMnO_4$ and KOH reacts at elevated temperatures and forms dark green unstable K_2MnO_4, which undergoes spontaneous, slow decomposition to MnO_2:

$$4\,KMnO_4 + 4\,KOH \rightarrow 4\,K_2MnO_4 + 2\,H_2O + O_2 \quad (1)$$

$$2\,K_2MnO_4 + 2\,H_2O \rightarrow 2\,MnO_2 + 4\,KOH + O_2 \quad (2)$$

The reaction suspension absorbs ultrasonic waves, causing a heating of the solution to a suitable reaction temperature above 60°C, which is necessary for the formation of alkali metal manganates and which also accelerates its decomposition according to Equations 1 and 2. Manganate solutions can intercalate IAGs, and oxygen species formed in these reactions could be helpful for exfoliation. The exfoliation processes based on longitudinal and stationary ultrasonic waves take place simultaneously. This method has proven to be very useful as a general method for exfoliation of available materials with a lamellar structure.

The raw samples of molybdenite and tungstenite correspond to the card numbers 96-900-9145 and 96-901-2192 of the crystallography open database (COD), as seen in Figure 2. The inset presents the XRD spectra of the exfoliated MoS_2 and WS_2, recorded in a water suspension between two Mylar foils to avoid drying and restacking. Figure 3 shows the XRD patterns of the synthesized bulk h-BN, h-BCN, and g-C_3N_4 used for exfoliation. The bulk h-BN showed a diffraction line with 2Θ at 25.5° (002) and one line with a lower intensity at 42.7° (100), which are indexed on JC PDF card number 85-1068. The h-BCN sample corresponds to the JC PDF card number 52-0233, and the diffraction pattern consisted of three weak peaks at 26.4° (002), 42.3° (100), and 54.8° (004). The g-C_3N_4 possesses two diffraction lines, and it is widely accepted that g-C_3N_4 is based on tri-*s*-triazine building blocks [40]. The strongest peak at 27.65° is a characteristic interlayer stacking peak of aromatic systems, indexed for graphitic materials as the (002) peak. The small angle peak at 13.01°, corresponding to an interplanar distance of 0.676 nm, is indexed as (100), which is associated with interlayer stacking [35].

When the exfoliated samples were dried, all of the characteristic peaks for raw IAGs - MoS_2, WS_2, h-BN, h-BCN, and g-C_3N_4 - reappear. The positions of the diffraction line (002) with 2Θ for MoS_2 and WS_2 at 14.3°, for h-BN and h-BCN at 26.0°, and for g-C_3N_4 at 28.0° were used to calculate the particle size and interlayer spacing (d_{002}). To compare the crystal structures of the synthesized bulk and exfoliated samples, the crystallite sizes and interlayer spacing (d_{002}) were calculated using
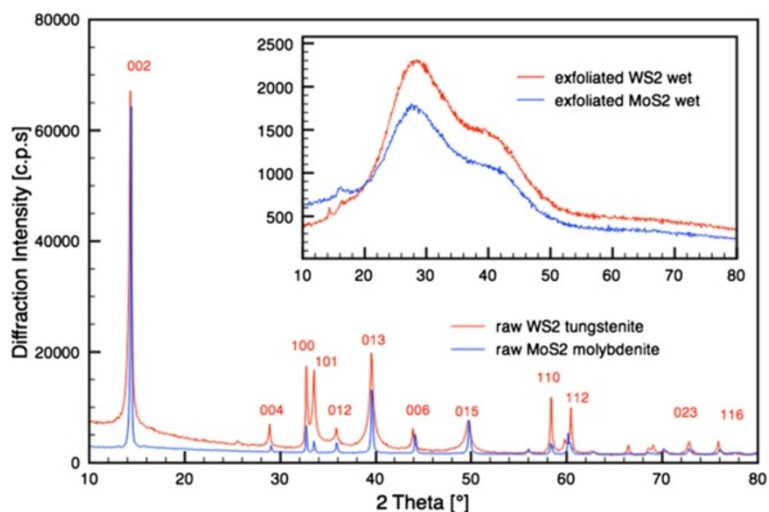
Figure 2 XRD patterns of raw molybdenite MoS$_2$ and tungstenite. The inset shows the patterns of the ultrasound-exfoliated samples.

the Scherrer equation in the High-Score Plus v. 3.0a program. The results are presented in Additional file 1: Table S1.

The dependence of the interlayer distance (d_{002}) on the degree of unidimensional disorder, γ, in graphite-like BN was determined. It was established that in the perfectly ordered structure with $\gamma = 0$, d_{002} is equal to 0.333 nm. The value of d_{002} increased uniformly with an increase in γ; for $\gamma = 1$, the determined value of d_{002} is 0.343 nm [41]. The MoS$_2$, WS$_2$, and g-C$_3$N$_4$ interlayer spacing was 0.313 nm. The h-BCN interlayer spacing was determined to be approximately 0.335 nm [42] or approximately 0.35 nm [43], which is close to the typical d_{002} spacing in hexagonal structures and slightly longer than the distance in h-BN and graphite. In our case, the interlayer spacing

was calculated to be 0.349 nm for bulk h-BN (1:3) and 0.341 nm for bulk h-BCN.

After exfoliation, wider interlayer spacings were expected, as was observed in the exfoliation of graphite [29]. However, as is evident from Additional file 1: Table S1, the value of d_{002}, depending upon the number of layers, decreases to a value of approximately 0.31 nm. Banhart [44] observed a similar reduction in the spacing of graphene layers in carbon onions and interpreted the reduction as a compression and the transition of orbitals from sp^2 to sp^3. In the Fe$_3$C encapsulated inside chain-like carbon nanocapsules, the smaller spacing of the graphene layers is related to the Fe$_3$C particle. The bonding between the graphene layers and the Fe$_3$C particle may contribute to the transition of orbitals from sp^2 to sp^3. The same
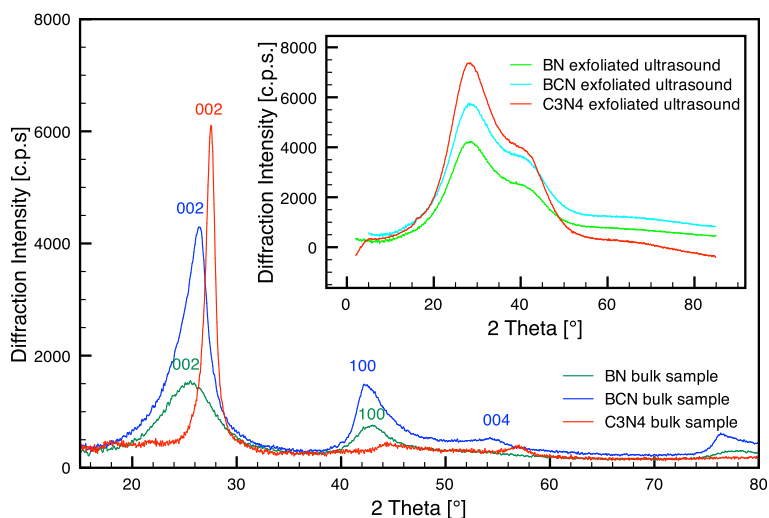

Figure 3 XRD patterns of bulk synthetic samples of h-BN, h-BCN, and g-C$_3$N$_4$. The inset shows the patterns of the ultrasound-exfoliated samples.

effect - decreasing of *d*-spacing - was due to the interaction of the energetic particles with the carbon nanostructures [45].

In our case, the reduction of *d*-spacing is most likely due to the compression pressure caused by the collapse of the cavitation bubbles. Additional file 1: Figures S1 and S3 show high-resolution transmission electron microscopy (HRTEM) micrographs of exfoliated MoS_2 and WS_2 sheets that were obtained using ultrasound-assisted exfoliation. The *d*-spacing of MoS_2 (0.639 nm) and WS_2 (1.195 nm) corresponds with the (002) plane of the PDF 02-1133 card and the (205) plane of the PDF 08-0237 card, respectively.

Using the Miller-Bravais indices (*hkil*) for layered materials such as graphene, each set of diffraction spots exhibited an inner hexagon that corresponds with a (1-110) index and an outer hexagon that corresponds

with a (1-210) index. The intensity profiles of the graphene diffraction patterns could therefore be used to determine the number of layers in the graphite sheet. The relative intensities of the diffraction spots in the inner and outer hexagons were shown to be equivalent to single-layer graphene, while the relative intensities of the spots in the outer hexagon were shown to be twice that of the spots in the inner hexagon for bilayer graphene [46]. The SAED of the prepared IAGs (MoS_2 and WS_2) are presented in Additional file 1: Figures S2 and S4, which shows the as-expected typical sixfold symmetry for the hexagonal forms of IAGs. The intensity of a line section through the (1-210), (0-110), (-1010), and (-2110) spots is shown in the inset figure. The inner (0-110)- and (-1010)-type reflections are more intense than the outer (1-210)- and (-2110)-type reflections, which is consistent with isolated single layers of IAGs.
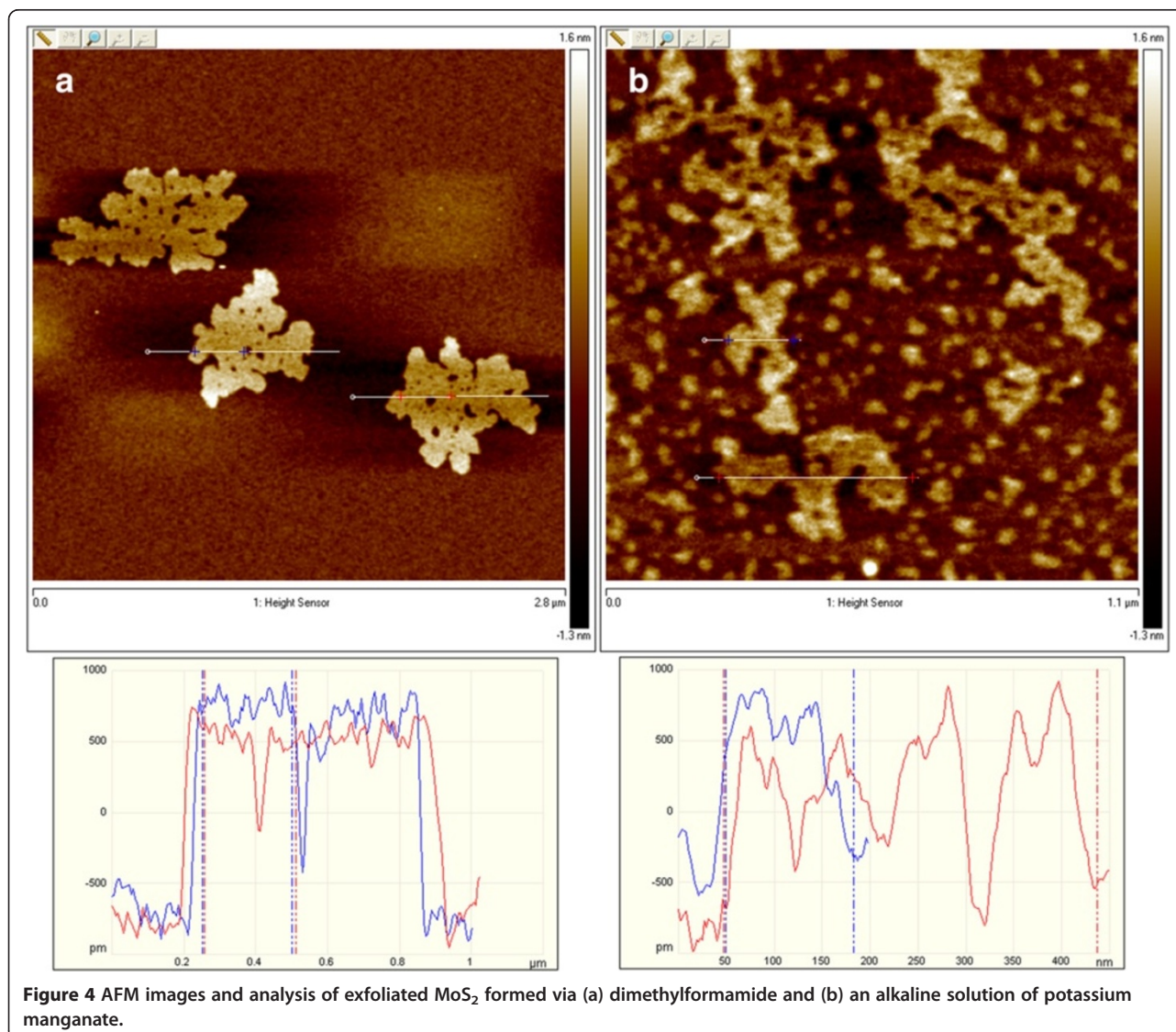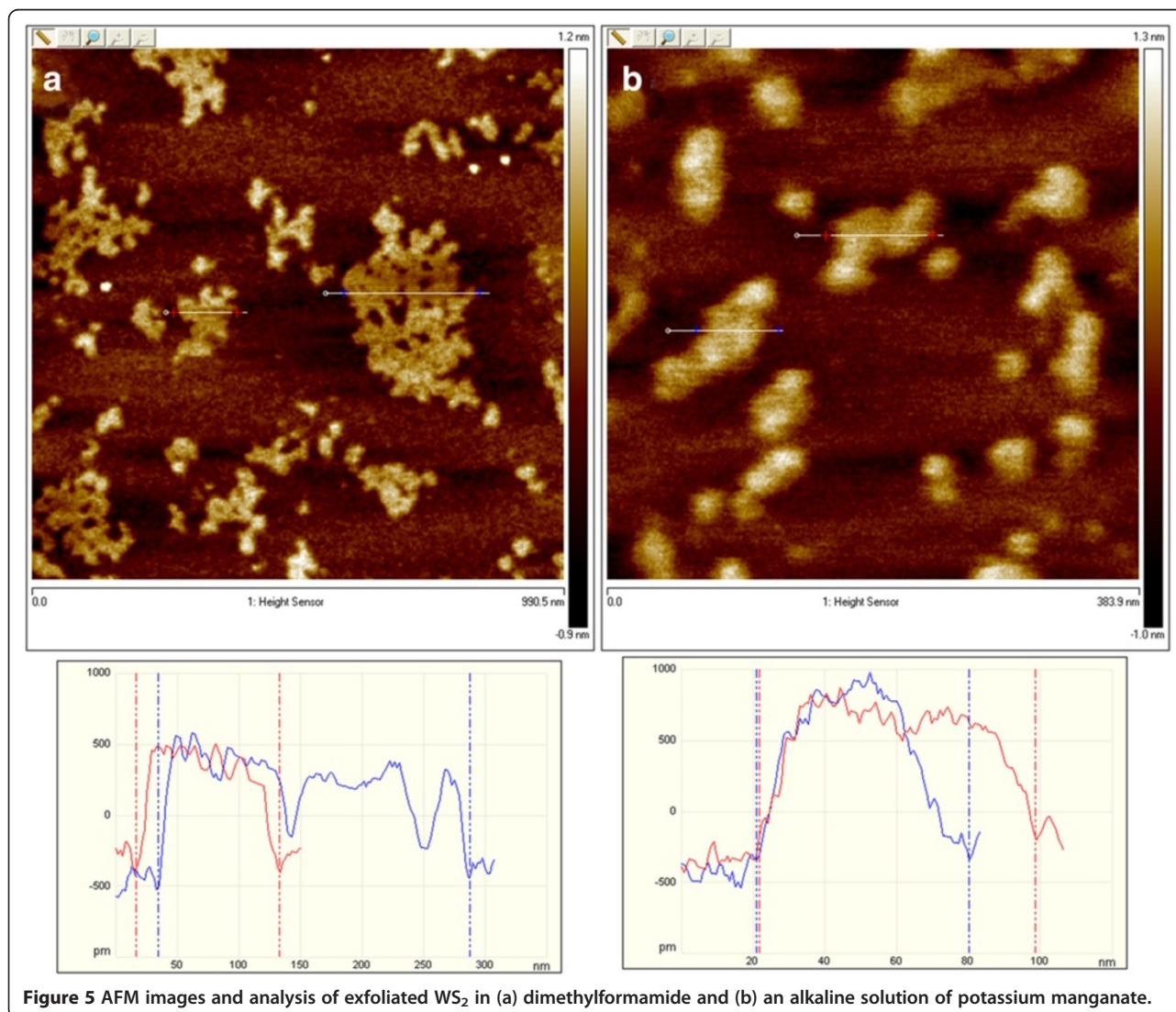

Figure 4 AFM images and analysis of exfoliated MoS₂ formed via (a) dimethylformamide and (b) an alkaline solution of potassium manganate.

HRTEM observations of the ultrasound-exfoliated h-BN and h-BCN (see Additional file 1: Figures S5 and S7) revealed a small fraction of an amorphous part in the material. By careful examination, we have found that besides the boron nitride nanocrystals with a size of approximately 2 to 3 nm, some amorphous domains were formed with an average diameter of 5 to 10 nm and are inter-layered within the crystalline domain. The d-spacings of the crystalline domains were found to be 0.345 and 0.366 nm for h-BN and h-BCN, respectively, which correspond to the (002) plane. Additional file 1: Figures S6 and S8 present SAED of synthesized h-BN and h-BCN, which confirms the results from XRD diffraction analysis.

TEM images and SAED of g-C_3N_4 are shown in Additional file 1: Figures S9 and S10. The sixfold symmetry is clearly visible, and Bravais-Miller ($hkil$) indices are used to label the diffraction peaks. Interestingly, the diffraction intensities of the inner spots (0-110) and (-1010) are always lower than those of the outer spots (1-210) and (-2110). This type of reflection would correspond to bilayer g-C_3N_4 [47].

The definite proof of the presence of exfoliated IAG sheets was provided by AFM, which can determine the height and therefore the number of layers. Figures 4 and 5 show the typical tapping-mode AFM images of MoS_2 and WS_2 exfoliated sheets using (a) dimethylformamide (DMF) and (b) the mixture of $KMnO_4$ and KOH, which were deposited on a mica substrate. Cross-sectional analysis shows that the exfoliated MoS_2 sheet had a thickness of approximately 0.7 nm and a lateral size of approximately 0.5 × 1.0 μm. Similarly, the exfoliated WS_2 sheets possess a thickness of approximately 0.7 to 1 nm and a size of 80 to 100 nm. Thus, the conclusion from the observation of exfoliated WS_2 and MoS_2 is that single-layered sheets were achieved. This result is consistent with

Figure 5 AFM images and analysis of exfoliated WS_2 in (a) dimethylformamide and (b) an alkaline solution of potassium manganate.

the aforementioned TEM observation. Figures 6 and 7 present AFM images of ultrasonically exfoliated h-BN and h-BCN. As seen in these figures, power ultrasound provided very uniformly delaminated materials. The analysis of the height profiles of both h-BN and h-BCN indicated

that the thickness of the sheets is approximately 1 nm. This would note that the treated bulk-layered material provided mostly single (or double) sheets [48]. An important fact to emphasize is the height uniformity of the particles (clearly visible from the color scale) in the selected
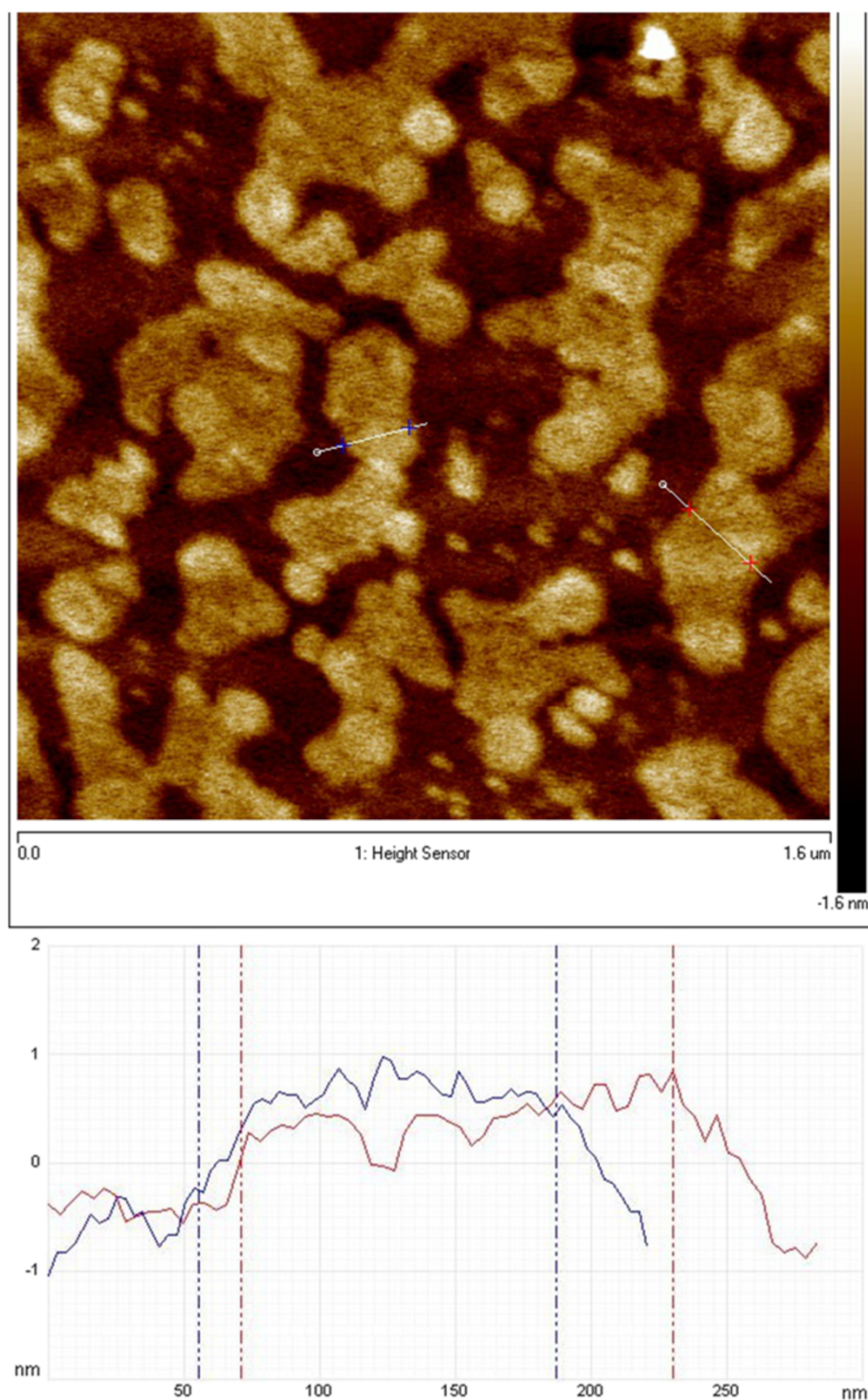
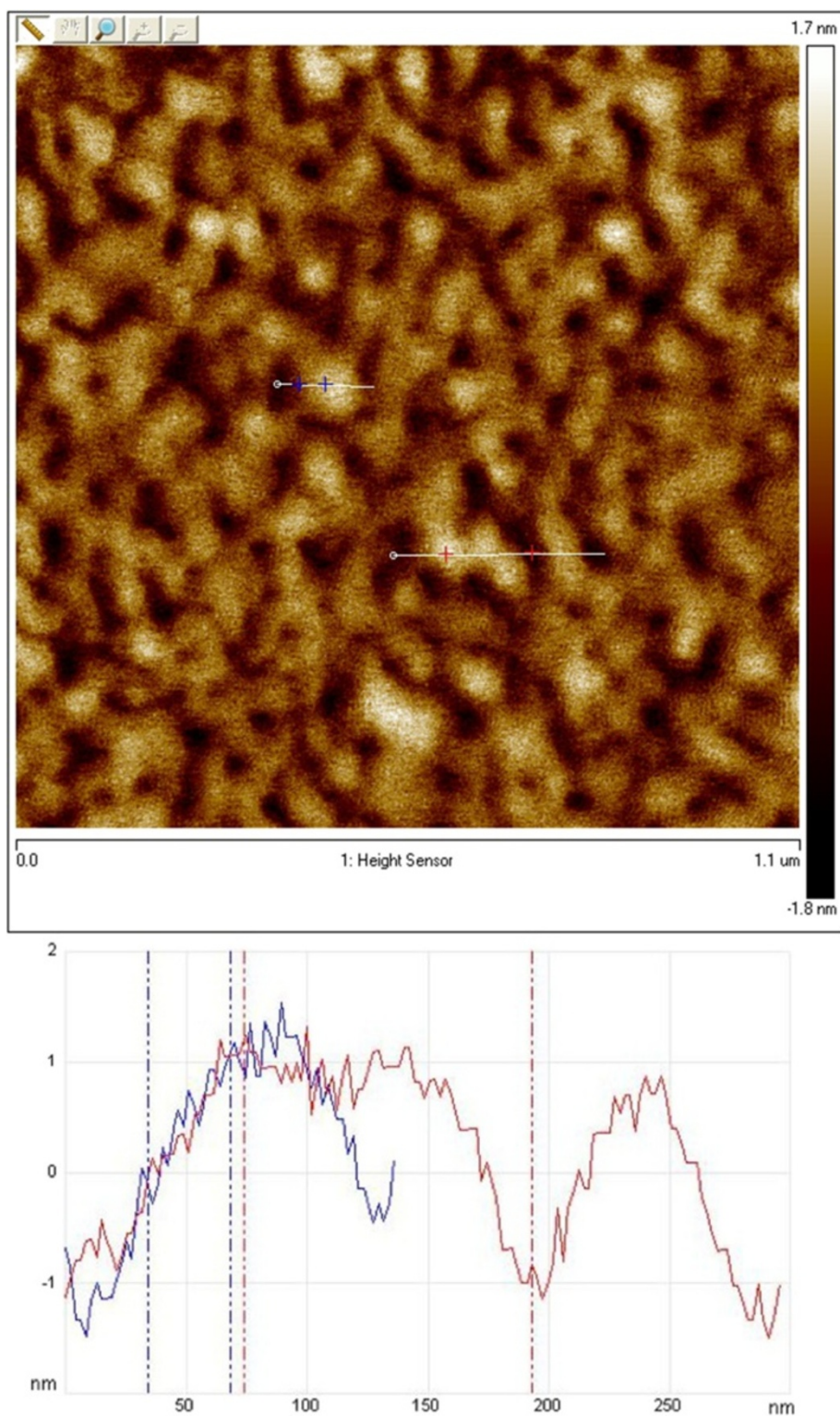**Figure 6 AFM image and analysis of exfoliated h-BN.**

Figure 7 AFM image and analysis of exfoliated h-BCN.

spots of the samples in the AFM analysis. Power ultrasound can therefore be suitable for larger scale production of homogeneous samples. The quality of the exfoliation by

ultrasonic waves is evident in the comparison with chemically delaminated BN produced by the modified Hummers method [36]. As seen in the picture from the

AFM microscope (see Figure 8), chemical delamination provided mostly 10-nm-thick particles of h-BN.

The AFM image of exfoliated g-C_3N_4 in ethylene glycol is shown in Figure 9. From the image analysis, it is clear that the exfoliated sample formed particles of 60 to 80 nm in size with heights of approximately 1.6 nm. A high-resolution AFM image is presented in Figure 10. Cross-sectional analysis showed that the
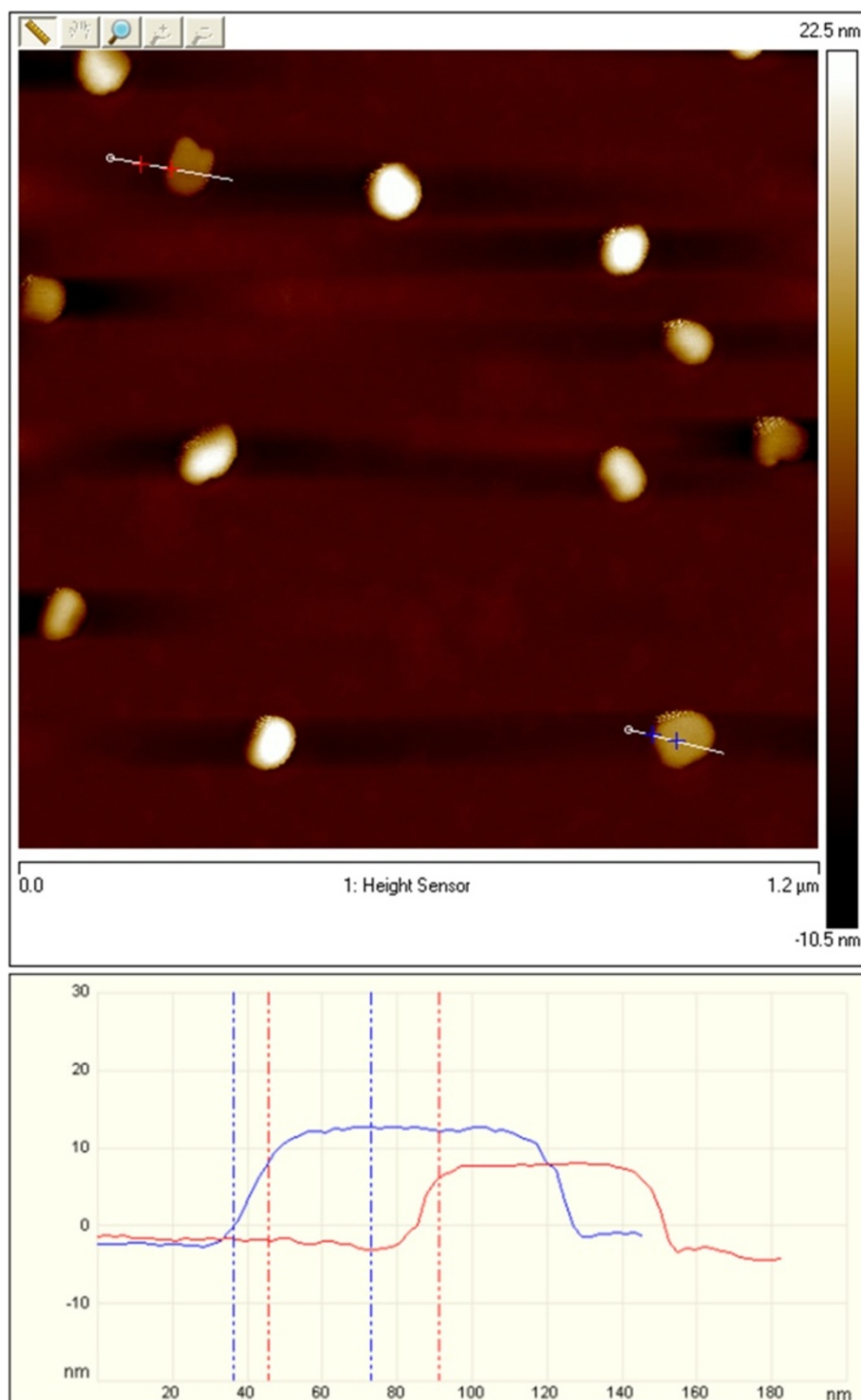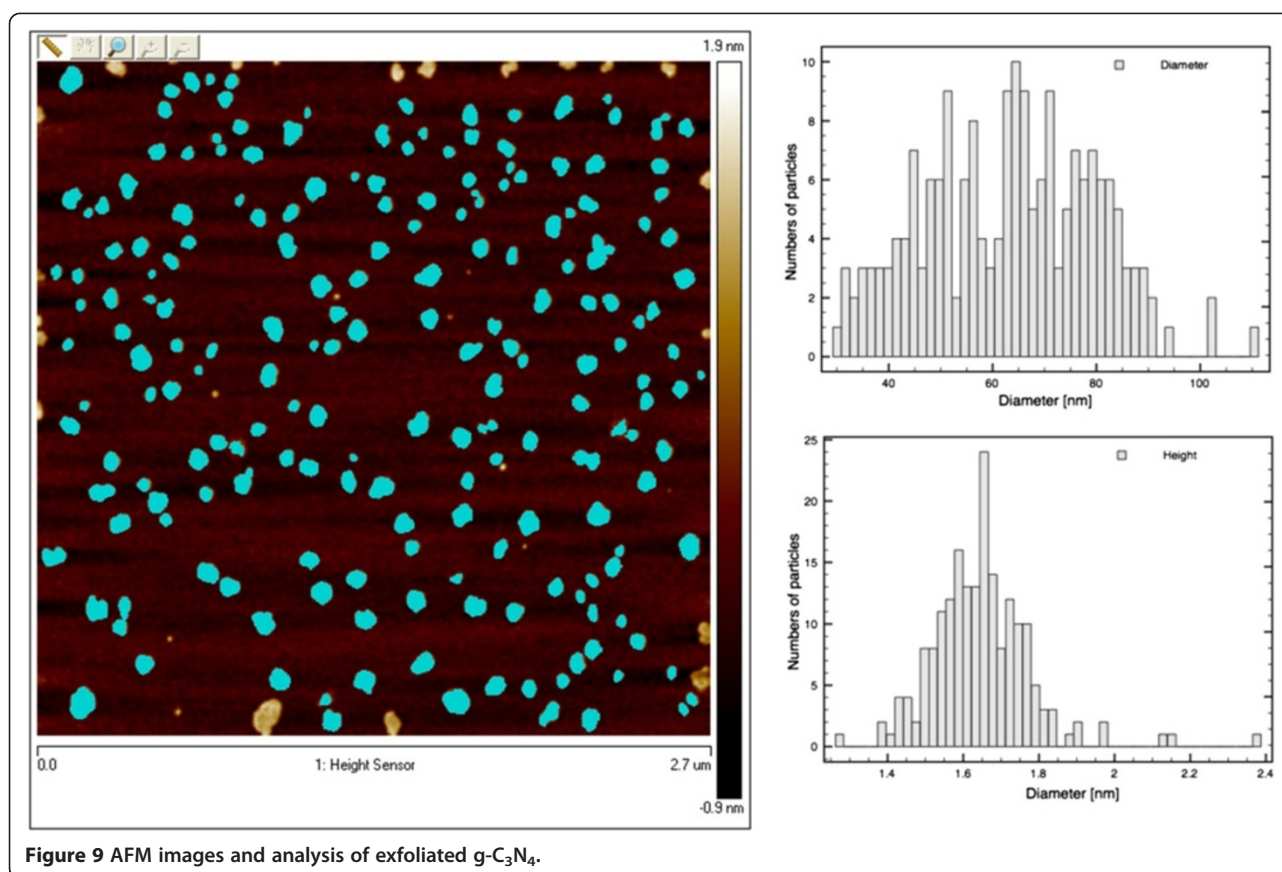

Figure 8 AFM image and analysis of chemically exfoliated h-BN.

Figure 9 AFM images and analysis of exfoliated g-C$_3$N$_4$.

exfoliated g-C$_3$N$_4$ sheet has a thickness of approximately 0.1 nm and the sheet has a size of approximately 80 × 100 nm. These results correspond with the results from SAED for bilayer particles.

Zhi et al. [49] presented exfoliation of bulk h-BN in dimethylformamide by sonication for 10 h with subsequent centrifugation to remove residual large-sized BN particles. Approximately 0.5 to 1 mg of h-BN nanosheets could be routinely obtained from 1 g of the bulk h-BN powder; this corresponds to a yield of exfoliation of approximately 1%. The liquid exfoliation of layered materials [50,51] provided similar yields. All the aforementioned cited exfoliation methods improve yields by countless repetition of exfoliation with the necessary intermediate operations (centrifugation) that isolate exfoliated products from the initial suspension. The resulting product is a diluted dispersion of the nanosheets in a suitable solvent.

Here, the reported method using the high-power ultrasound produced a concentrated colloidal dispersion of nanosheets by one-step sonication; the product possesses a relatively homogeneous distribution of the few- or monolayers, as seen in the AFM images. By this method, large quantities of the colloidal dispersion of nanosheets are readily available as a precursor (for example, for the preparation of composites) and can be produced in a short time. Using an alkaline medium to prepare exfoliated IAGs could be an important shift in the preparation of these materials. Using alkaline solutions for ultrasonic preparation could exclude hydrophobic organic solvents and consequently contamination by organic residuals and undesired functionalization of the nanosheets. Furthermore, the product prepared in an alkaline environment could possess a different reactivity, thanks to possibly different composition of surface functional groups. However, further investigations of this proposed method are necessary.

Conclusions

The method of exfoliation in a pressurized batch ultrasonic reactor allows for the preparation of few- and monolayered colloidal dispersions of IAG particles without intercalation. The quality and quantity of the exfoliation depends upon appropriate selection of the reaction conditions (intensity of ultrasound, the reaction time, the pressure in the reactor, etc.). Strong aprotic solvents (NMP, DMF, DMSO, etc.) are used for the preparation of monolayered IAGs in a hydrophobic environment. The method of exfoliation of IAGs that is based on the intercalation of potassium manganate in an alkaline
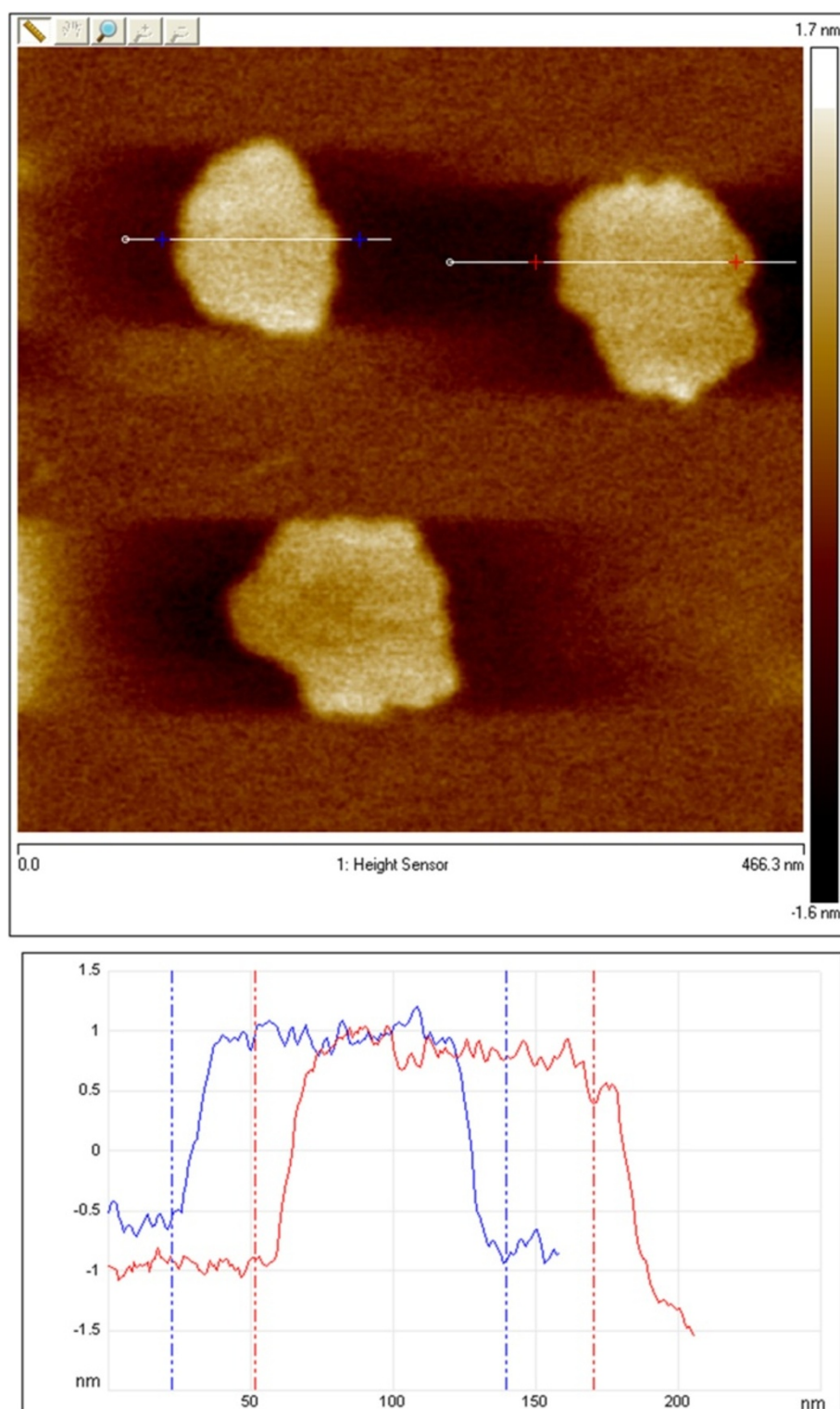
Figure 10 High-resolution AFM image and analysis of exfoliated g-C$_3$N$_4$.

environment in the presence of high-intensity ultrasound is suitable for hydrophilic applications with a good dispersibility of the IAGs in water. This non-oxidative method allows for the preparation of exfoliated IAGs of high purity with a minimum content of undesirable functional groups.

Additional file

Additional file 1: Supplement information Table S1. Integral breath, d-spacing and crystallite size of prepared samples IAGs. **Figure S1.** HRTEM of exfoliated MoS2. **Figure S2.** SAED of exfoliated MoS2. **Figure S3.** HRTEM of exfoliated WS2. **Figure S4.** SAED of exfoliated WS2. **Figure S5.** HRTEM of exfoliated h-BN. **Figure S6.** SAED of exfoliated h-BN. **Figure S7.** HRTEM of exfoliated h-BCN. **Figure S8.** SAED of exfoliated h-BCN. **Figure S9.** TEM of exfoliated g-C_3N_4. **Figure S10.** SAED of exfoliated g-C_3N_4.

Competing interests

The authors declare that they have no competing interests.

Authors' contributions

VS was the main author of the work, performed the syntheses, and coordinated all characterization. MS was responsible for the electron microscopy, JH for the AFM microscopy, and PE for the XRD measurement. All authors read and approved the final manuscript.

Author details

[1]Materials Chemistry Department, Institute of Inorganic Chemistry AS CR, v.v.i., Řež 250 68, Czech Republic. [2]Faculty of Environment, J.E. Purkyně University in Ústí nad Labem, Ústí nad Labem 400 96, Czech Republic.

References

1. Novoselov KS: **Graphene: materials in the flatland (Nobel Lecture).** *Angew Chem Int Ed* 2011, **50**:6986–7002.
2. Eda G, Yamaguchi H, Voiry D, Fujita T, Chen M, Chhowalla M: **Photoluminescence from chemically exfoliated MoS₂.** *Nano Lett* 2011, **11**:5111–5116.
3. Castellanos-Gomez A, Poot M, Steele GA, van der Zant HSJ, Agrait N, Rubio-Bollinger G: **Mechanical properties of freely suspended semiconducting graphene-like layers based on MoS₂.** *Nanoscale Res Lett* 2012, **7**:1–4.
4. Liu LT, Kumar SB, Ouyang Y, Guo J: **Performance limits of monolayer transition metal dichalcogenide transistors.** *IEEE Trans Electron Dev* 2011, **58**:3042–3047.
5. Li LH, Petravic M, Cowie BCC, Xing T, Peter R, Chen Y, Si C, Duan WH: **High-resolution x-ray absorption studies of core excitons in hexagonal boron nitride.** *Appl Phys Lett* 2012:604–608.
6. Novoselov KS, Jiang D, Schedin F, Booth TJ, Khotkevich VV, Morozov SV, Geim AK: **Two-dimensional atomic crystals.** *Proc Natl Acad Sci U S A* 2005, **102**:10451–10453.
7. Joensen P, Frindt RF, Morrison SR: **Single-layer MoS₂.** *Mater Res Bull* 1986, **21**:457–461.
8. Miremadi BK, Cowan T, Morrison SR: **New structures from exfoliated MoS₂.** *J Appl Phys* 1991, **69**:6373–6379.
9. Miremadi BK, Morrison SR: **Exfoliated MoS₂ temperature programmed desorption.** *Surf Sci* 1986, **173**:605–617.
10. Yao Y, Lin Z, Li Z, Song X, Moon K-S, Wong C-P: **Large-scale production of two-dimensional nanosheets.** *J Mater Chem* 2012, **22**:13494–13499.
11. Miremadi BK, Morrison SR: **The intercalation and exfoliation of tungsten disulfide.** *J Appl Phys* 1988, **63**:4970–4974.
12. Yang D, Frindt RF: **Li-intercalation and exfoliation of WS₂.** *J Phys Chem Solid* 1996, **57**:1113–1116.
13. Gordon RA, Yang D, Crozier ED, Jiang DT, Frindt RF: **Structures of exfoliated single layers of WS₂, MoS₂, and MoSe₂ in aqueous suspension.** *Phys Rev B* 2002, **65**:125407–1254011.
14. Rao CNR, Nag A: **Inorganic analogues of graphene.** *Eur J Inorg Chem* 2010, **2010**:4244–4250.
15. Zhou K-G, Mao N-N, Wang H-X, Peng Y, Zhang H-L: **A mixed-solvent strategy for efficient exfoliation of inorganic graphene analogues.** *Angew Chem Int Ed* 2011, **50**:10839–10842.
16. Wang Y, Zhou C, Wang W, Zhao Y: **Preparation of two dimensional atomic crystals BN, WS₂, and MoS₂ by supercritical CO₂ assisted with ultrasound.** *Ind Eng Chem Res* 2013, **52**(11):4379–4382.
17. Warner JH, Rummeli MH, Bachmatiuk A, Buchner B: **Atomic resolution imaging and topography of boron nitride sheets produced by chemical exfoliation.** *ACS Nano* 2010, **4**:1299–1304.
18. Lin Y, Williams TV, Xu T-B, Cao W, Elsayed-Ali HE, Connell JW: **Aqueous dispersions of few-layered and monolayered hexagonal boron nitride nanosheets from sonication-assisted hydrolysis: critical role of water.** *J Phys Chem C* 2011, **115**:2679–2685.
19. Sun G, Wu Q, Hu Q, Yu D: **Chemical reduction synthesis of hexagonal B-C-N compound.** *J Inorg Mater* 2008, **23**:1067–1069.
20. Wang S, Zhang L, Xia Z, Roy A, Chang DW, Baek J-B, Dai L: **BCN graphene as efficient metal-free electrocatalyst for the oxygen reduction reaction.** *Angew Chem Int Ed* 2012, **51**:4209–4212.
21. Hernandez Y, Nicolosi V, Lotya M, Blighe FM, Sun ZY, De S, McGovern IT, Holland B, Byrne M, Gun'ko YK, Boland JJ, Niraj P, Duesberg G, Krishnamurthy S, Goodhue R, Hutchison J, Scardaci V, Ferrari AC, Coleman JN: **High-yield production of graphene by liquid-phase exfoliation of graphite.** *Nat Nanotechnol* 2008, **3**:563–568.
22. Weiss K, Phillips JM: **Calculated specific surface energy of molybdenite (MoS₂).** *Phys Rev B* 1976, **14**:5392–5395.
23. Suslick KS, Eddingsaas NC, Flannigan DJ, Hopkins SD, Xu H: **Extreme conditions during multibubble cavitation: sonoluminescence as a spectroscopic probe.** *Ultrason Sonochem* 2011, **18**:842–846.
24. Atchley AA, Frizzell LA, Apfel RE, Holland CK, Madanshetty S, Roy RA: **Thresholds for cavitation produced in water by pulsed ultrasound.** *Ultrasonics* 1988, **26**:280–285.
25. Sponer J: **Dependence of the cavitation threshold on the ultrasonic frequency.** *Czechoslov J Phys* 1990, **40**:1123–1132.
26. Stengl V, Subrt J: **Power ultrasound and its applications.** *Chem List* 2004, **98**:324–327.
27. Stengl V, Subrt J, Bakardjieva S: **Chemically modified mica.** *Chem List* 2002, **97**:45–48.
28. Stengl V, Subrt J, Karas M: **Method of delamination of layered minerals and materials.** *CZ 290420 B6* 2002.
29. Stengl V: **Preparation of graphene by using an intense cavitation field in a pressurized ultrasonic reactor.** *Chemistry* 2012, **18**:14047–14054.
30. Stengl V, Popelkova D, Vlacil P: **TiO₂-graphene nanocomposite as high performace photocatalysts.** *J Phys Chem C* 2011, **115**:25209–25218.
31. Stengl V, Bakardjieva S, Grygar TM, Bludska J, Kormunda M: **TiO₂-graphene oxide nanocomposite as advanced photocatalytic materials.** *Chem Cent J* 2013, **7**:1–12.
32. Stengl V, Cerny Z, Bludska J: **Method of preparation of single-layer particles.** PV 2013-620. Czech rep; 2013.
33. Nag A, Raidongia K, Hembram KPSS, Datta R, Waghmare UV, Rao CNR: **Graphene analogues of BN: novel synthesis and properties.** *ACS Nano* 2010, **4**:1539–1544.
34. He JL, Tian YJ, Yu DL, Wang TS, Xiao FR, Li AD, Li DC, Peng YG, Li L: **Chemical synthesis of crystalline hexagonal B-C-N compound.** *J Mater Sci Lett* 2061–2063, **2000**:19.
35. Yan SC, Li ZS, Zou ZG: **Photodegradation performance of g-C₃N₄ fabricated by directly heating melamine.** *Langmuir* 2009, **25**:10397–10401.
36. Hummers WS, Offeman RE: **Preparation of graphitic oxide.** *J Am Chem Soc* 1958, **80**:1339–1339.
37. JCPDS: *JCPDS PDF-2 Database. International Centre for Diffraction Data.* Newtown Square: JCPDS; 2004.
38. Sakintuna B, Yürüm Y, Çetinkaya S: **Evolution of carbon microstructures during the pyrolysis of Turkish Elbistan lignite in the temperature range 700 – 1000°C.** *Energy Fuel* 2004, **18**:883–888.
39. Saner B, Okkay F, Yurum Y: **Utilization of multiple graphene layers in fuel cells. 1. An improved technique for the exfoliation of graphene-based nanosheets from graphite.** *Fuel* 2010, **89**:1903–1910.
40. Thomas A, Fischer A, Goettmann F, Antonietti M, Muller J-O, Schlogl R, Carlsson JM: **Graphitic carbon nitride materials: variation of structure and morphology and their use as metal-free catalysts.** *J Mater Chem* 2008, **18**:4893–4908.

41. Kurdyumov AV, Zelyavskii VB, Ostrovskaya NF, Borimchuk NI, Yarosh VV, Gromyko SN, Yarosh NV: **Nature of the real structure of graphite-like BN and its transformation into a wurtsite modification under impact compression.** *Powder Metall Met Ceram* 1995, **33**:501–504.
42. Sun G, Gao F, Hou L: **Fabrication of boron carbonitride (BCN) nanotubes and giant fullerene cages.** *Can J Chem* 2010, **88**:1256–1261.
43. Krause M, Bedel L, Taupeau A, Kreissig U, Munnik F, Abrasonis G, Kolitsch A, Radnoczi G, Czigany Z, Vanhulsel A: **Structural and mechanical characterization of BC$_x$N$_y$ thin films deposited by pulsed reactive magnetron sputtering.** *Thin Solid Films* 2009, **518**:77–83.
44. Banhart F: **Irradiation effects in carbon nanostructures.** *Rep Prog Phys* 1999, **62**:1181.
45. Tokushi K, Kunichi M, Daisuke M: **Synthesis of carbon nanocapsules and nanotubes using Fe-doped fullerene nanowhiskers.** *J Nanotechnology* 2012, **2012**:1181–1184.
46. Dato A, Radmilovic V, Lee Z, Phillips J, Frenklach M: **Substrate-free gas-phase synthesis of graphene sheets.** *Nano Lett* 2012–2016, **2008**:8.
47. Lee S, Lee K, Zhong Z: **Wafer scale homogeneous bilayer graphene films by chemical vapor deposition.** *Nano Lett* 2010, **10**:4702–4707.
48. Lee C, Li QY, Kalb W, Liu XZ, Berger H, Carpick RW, Hone J: **Frictional characteristics of atomically thin sheets.** *Science* 2010, **328**:76–80.
49. Zhi C, Bando Y, Tang C, Kuwahara H, Golberg D: **Large-scale fabrication of boron nitride nanosheets and their utilization in polymeric composites with improved thermal and mechanical properties.** *Adv Mater* 2009, **21**:2889–2893.
50. Coleman JN, Lotya M, O'Neill A, Bergin SD, King PJ, Khan U, Young K, Gaucher A, De S, Smith RJ, Shvets IV, Arora SK, Stanton G, Kim H-Y, Lee K, Kim GT, Duesberg GS, Hallam T, Boland JJ, Wang JJ, Donegan JF, Grunlan JC, Moriarty G, Shmeliov A, Nicholls RJ, Perkins JM, Grieveson EM, Theuwissen K, McComb DW, Nellist PD, *et al*: **Two-dimensional nanosheets produced by liquid exfoliation of layered materials.** *Science* 2011, **331**:568–571.
51. Nicolosi V, Chhowalla M, Kanatzidis MG, Strano MS, Coleman JN: **Liquid exfoliation of layered materials.** *Science* 2013, **340**:1420–1424.